Renewable and Sustainable Energy Reviews 134 (2020) 110336

Contents lists available at ScienceDirect

Renewable and Sustainable Energy Reviews

journal homepage: http://www.elsevier.com/locate/rser

Actively heated fiber optics based thermal response test: A field demonstration

Bo Zhang [a], Kai Gu [a,b,*], Bin Shi [a,**], Chun Liu [a], Peter Bayer [c], Guangqing Wei [d], Xülong Gong [e], Lei Yang [e]

[a] School of Earth Sciences and Engineering, Nanjing University, Nanjing, 210023, China
[b] Nanjing University High-Tech Institute at Suzhou, Suzhou, 215123, China
[c] Institute of Geosciences and Geography, Martin-Luther University Halle-Wittenberg, Von Seckendorff-Platz 4, 06120, Halle (Saale), Germany
[d] Suzhou Nanzee Sensing Technology Co.Ltd., Suzhou, 215123, China
[e] Key Laboratory of Earth Fissures Geological Disaster, Ministry of Land and Resources (Geological Survey of Jiangsu Province), Nanjing, 210018, China

ARTICLE INFO

Keywords:
Shallow geothermal energy
Thermal response test
Actively heated fiber optics
In-situ test
Distributed temperature sensing
Heating wires

ABSTRACT

Accurate estimation of thermal ground properties is needed to optimally apply shallow geothermal energy technologies, which are of growing importance for the heating and cooling sector. A special challenge is posed by the often significant heterogeneity and variability of the geological media at a site. As an innovative investigation method, here the focus is on the actively heated fiber optics based thermal response test (ATRT). A type of copper mesh heated optical cable (CMHC), which both serves as a heating source and a temperature sensing cable, was applied in the field in a borehole. By inducing the electric current to the cable at a relatively low power of 26 W/m, the in-situ heating process was recorded at high depth resolution. This information serves to infer the thermal conductivity distribution along the borehole. The presented field experience reveals that the temperature rise in the early phase of the test should not be used due to initial heat accumulation caused by the outer jacket of the CMHC. The comparison of these results with those of a conventional thermal response test (TRT) and a distributed thermal response test (DTRT) in the same borehole confirmed that the ATRT result is reliable (with a difference less than 5% and 1%, respectively), since this novel method affords much less energy and test time. Additionally, the ATRT result agrees well with ground thermal conductivities tested in the lab, which supports its potential as an advanced geothermal field investigation technique in the future.

1. Introduction

In the pursuit of sustainable development and the mitigation of climate change, shallow geothermal energy has been widely recognized as a type of clean energy with great potential [1–3]. Especially closed-loop systems, so-called borehole heat exchangers (BHEs) are applied, where plastic tubes are implemented in vertical boreholes tens to hundreds of meters deep, and a heat carrier fluid is circulated in the tubes to extract or inject heat in-situ. The performance of this technology strongly depends on the properties of the ground, which however are commonly variable and heterogeneous in natural geological media. For example, layered sediments often build upon the shallow subsurface, with different physical properties in each layer. Among the most relevant properties is the ambient ground thermal conductivity that controls the heat flux and thus the performance at the borehole.

To properly assess the shallow geothermal energy potential and for the correct design of BHE systems, accurate estimation of thermal ground properties is required [4–6]. The most conventional in-situ method used to evaluate the thermal conductivities of subsurface soils is the thermal response test (TRT), which was first proposed by Morgensen in 1983 [7]. In this method, the average thermal conductivity of the strata in a vertical borehole is calculated based on the recorded inlet and outlet water temperature trend (i.e. the thermal response of the ground) by performing a constant power water cycle in the transducer pipe for a specific time, usually up to several days. There have been numerous studies for the purpose of improving its application and the analysis of results, involving analytical or numerical simulation, which makes TRT a meanwhile mature field investigation technique [8–10].

* Corresponding author. School of Earth Sciences and Engineering, Nanjing University, Nanjing, 210023, China.
** Corresponding author.
E-mail addresses: gukai@nju.edu.cn (K. Gu), shibin@nju.edu.cn (B. Shi).

https://doi.org/10.1016/j.rser.2020.110336
Received 22 January 2020; Received in revised form 23 August 2020; Accepted 1 September 2020
Available online 9 September 2020
1364-0321/© 2020 Elsevier Ltd. All rights reserved.

Yet, there are still technical and economic challenges for TRTs, which led to the development of several novel methods for in-situ thermal conductivity evaluation.

This paper begins with a brief review on both conventional TRT and novel enhanced TRTs, in which the improvement requirements for TRTs are discussed. And the objective of this paper is to introduce a novel method employing actively heated fiber optics technique, with its novelty and advantages illustrated. A field demonstration was conducted in Changzhou, China. The interpretation of measured data is presented and the results are validated with the findings from conventional TRTs and laboratory data.

2. Literature review on TRT and advanced TRTs

TRT is a conventional method of thermal conductivity (λ) and thermal borehole resistance (R_b) of subsurface ground. Morgensen (1983) [7] first proposed a theoretical method to determine the thermal resistance of borehole through a fixed heat extraction rate to the borehole, which also can be used to estimate ground thermal conductivity. Since then, similar tests were reported but mostly used a fixed heat rate to the borehole rather than a fixed heat extraction rate [8]. TRT is typically performed on the vertical borehole heat exchanger (BHE), which is installed in a borehole. A fixed heat rate is applied to the borehole by circulating water heated with a certain power in BHE. To determine the thermal properties, different mathematical models of TRT on the explanation of the heat transfer process were reported. Line source model, cylindrical source model, and numerical model are the basic models commonly used [8,9].

Accurate calculation of thermal conductivity using mathematical models requires a proper selection of heating power and heating time, on which the discussion still ongoing. ASHARE [11] recommended 49.2–82 W/m for a minimum heating time of 36–48 h. While other suggested heating times are also reported, such as 12–20 h [12], 24 h [13], and 60 h [14]. Recently, Pasquier [15] used new first-order approximation models reduced the heating time from 72 to 3 h in five cases with heating power range of 60–70 W/m. In order to better estimate the thermal conductivity and improve the efficiency of ground source heat pump, ways to reduce the thermal borehole resistance have been continually reported [10,16–18], mainly referring to the geometry of BHEs, grouting materials, etc.

It should be noted that, the thermal conductivity derived by standard TRT interpretation is a bulk value assuming homogeneous conditions in the ground, and only by heat conduction. Hence, it neglects any vertical variation of the thermal properties of the ground, which may be crucial for predicting the long-term performance of the BHE. Also, it is an effective parameter that may be influenced by advection due to groundwater flow, which in sedimentary formations is often variable along the borehole [19]. With the development of the distributed temperature sensing technique (DTS) using optical fibers, the temperature variation along a fiber can be measured during the TRT. Based on this so-called distributed thermal response test (DTRT), the vertical trend of thermal conductivity in the borehole can be determined. Fujii et al. [20,21] installed an optical cable onto the external wall of the BHE pipes, and the estimated thermal conductivity distribution reflected the variability of the surrounding rock and the influence of groundwater flow. When applied to a field site, the DTRT average thermal conductivity was consistent with that derived by a conventional TRT.

Acuña et al. [22] put forward the DTRT by placing the optical fiber inside the BHE pipe, and they demonstrated how to calculate thermal conductivity and borehole thermal resistance along the borehole. The thermal resistance is introduced in practice to account for all early time effects from borehole devices, tubes, and grout. Acuña also performed DTRT with different types of BHEs [23–25], and the coaxial pipe-in-pipe BHEs is considered to significantly reduce the thermal borehole resistance compared to the U-pipe BHEs. Further studies revealed that groundwater flow is an important factor that affects the DTRT results by locally enhancing the heat transfer [9,26,27].

Both TRT and DTRT are based on circulating a warmed heat carrier fluid in the pipes of the borehole for several days. Instead, new methods using an actively heated optical fiber cable have been suggested [27,28]. Such methods use heating wires to replace the warmed heat carrier fluid as a heat source and also employ fiber optic techniques to measure the temperature variation along the borehole. Dornstädter et al. [29] introduced their so-called enhanced thermal response test (ETRT) by assembling a plurality of copper core cables and optical cables to form a hybrid optical cable, which is installed at the outer face of the U-pipes in a BHE. Huber and Arslan [30] conducted an ETRT in a 50 m borehole to evaluate the effect of groundwater flow on the test results. Vieira et al. [31] demonstrated that ETRT applications required less power and shortened test time in comparison to conventional TRTs. Other methods based on actively heated fiber optical cable have been reported as well. Freifeld et al. [32] presented a methodology that combines DTS with an electrical resistance heater to estimate thermal conductivity. The heater was a two-conductor 14 AWG direct cable parallel to the fiber-optical cable, energized the heater cable (16.8 W/m for 43 h followed by 20.5 W/m for 21 h) during heating. Raymond et al. [33–35] presented the application of a TRT with a reduced power source, which delivered data that was interpreted by numerical simulation. In their field test, heating cable sections were installed inside a single pipe of a BHE, as well as some read-only memory temperature sensors that were placed at different depths. Here, the duration of heat injection was more than 50 h. Luo et al. [36] concluded that their results (heating lasted over 3 days) were in good agreement with the lab test results of the drill core only in the absence of groundwater flow.

Recently, Vélez Márquez et al. [37] placed a continuous heating cable and a temperature sensing cable inside a U-pipe of the borehole for thermal response test and obtained a distributed thermal response test curve with a heating power of 9.9 W/m and a heating time of 135.6 h. The thermal conductivity was calculated for different depths and successfully compared with conventional TRT results. Galgaro et al. [38] assembled multiple copper core cables and optical cables to form a hybrid optical cable, which was U-shaped and fixed on a rigid long cylindrical rod in a grouted stand-alone observation borehole without pipes. In their presentation of preliminary results, the heating phase was only 5 h followed by several days of recovery phase that was monitored and used for interpretation. Modified TRTs based on the actively heated fiber optical cable have also been applied recently in related fields to measure soil moisture, groundwater flow rates, fissure flow, and wind speed [39–46].

It has been illustrated that TRTs using actively heated optical fiber cables can somehow save power and test time for in-situ thermal conductivity measurements, especially by positioning the hybrid cable at the outer surface of the pipe or directly installing the cable in a borehole [31,38]. Although there is a very small number of international publications, such setup has shown great potential [28]. Up to now, however, there are no standardized tools and procedures for this technique, which can be categorized as actively heated fiber optics based thermal response tests (ATRT). For example, electrically insulated heating elements inside the same cable construction (i.e. hybrid cables) can be more economical. However, the geometry then is not radially symmetric, and small differences in the separation between the heating element and optical fibers may cause unwanted temperature anomalies which are observable during heating [47]. For this direction, a novel method employing better designed hybrid cable should be developed and this method also should be technically and economically efficient.

3. Methodology

Aiming to fill the abovementioned gap, here actively heated fiber optics based thermal response test (ATRT) employs permanent special designed copper mesh heated optical cables (CMHC) was proposed. Rather than simply combining a heating cable and a sensing cable,

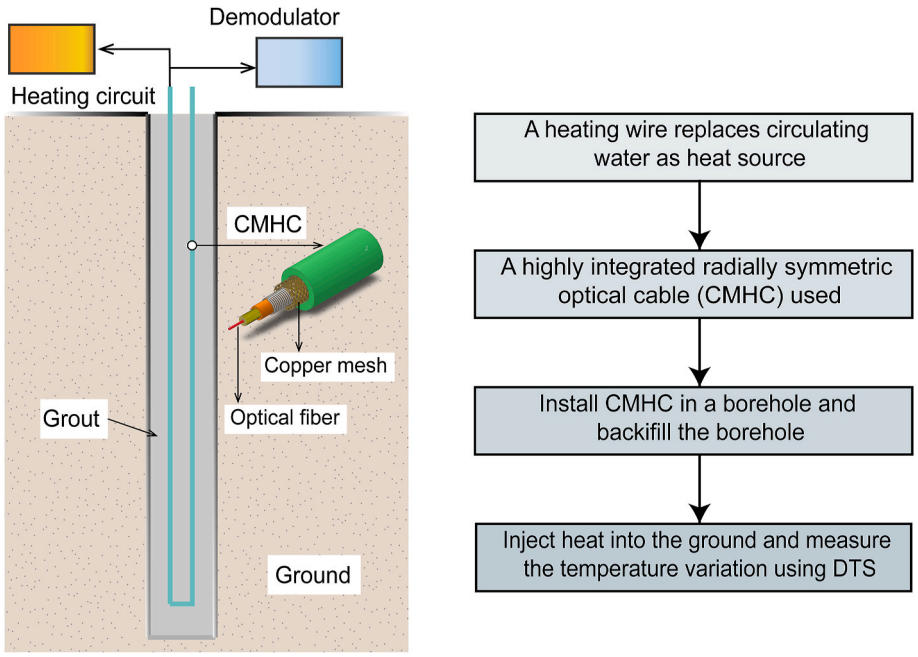

Fig. 1. The setup of actively heated fiber optics based thermal response test.

Table 1
Physical properties of the soils along the borehole.

Strata	Natural sample density ($g \cdot cm^{-3}$)	Bulk (dry) density ($g \cdot cm^{-3}$)	Void ratio
Clay	2.00–2.02	1.59–1.66	0.65–0.72
Silty Clay	1.92–2.10	1.47–1.77	0.53–0.86
Silt	1.95–2.04	1.55–1.71	0.57–0.74
Fine sand	1.89–1.97	1.47–1.56	0.72–0.84

Note: the number of soil samples of each type is more than three.

CMHC is a type of integrated cable that can serve as both a temperature sensing cable and a line heating source. The CMHC is radially symmetric, and the temperature measuring optical fiber is located at the center of the heated copper mesh layer. This structure can ensure uniform radial heat transfer. Fig. 1 shows the basic test setup of ATRT. CMHC can be either directly installed into the borehole in U-shape or fixed on the outside wall of BHE. Afterwards the borehole should be backfilled with grout as conventional TRTs. The heating circuit and optical fiber demodulator are both connected to CMHC. The heating circuit supplies a certain heating power inject into the strata, and the demodulator monitors the temperature changes through the optical fiber. The advantages of this proposed ATRT can be summarized as follows:

- Simple test setup. Only need to vertically install the CMHC and conventional BHE is not necessary.
- The highly integrated radially symmetrical optical cable CMHC is more in line with the assumption of the infinite line source model.
- Heat inject through heating wires can provide identical heating power along the borehole while circulating water may have nonuniformity.
- Good heating efficiency and temperature accuracy obtained by DTS can greatly reduce the energy cost and the duration time of the test.

3.1. Field site

The proposed ATRT was applied and demonstrated in the field. The field site consists of a 150 m deep vertical borehole located in Changzhou, Jiangsu province, China. The climate here can be categorized into the subtropical humid climate (Cfa subtype) according to the Köppen classification [48]. Generally, this area is considered to have above-average terrestrial heat-flow density [49]. Regarding to the geological background, this area belongs to the alluvial plain in the middle and lower reaches of the Yangtze River, where variable groundwater flow is present at shallow depth. The groundwater level was 1.3 m below the ground surface. The upper 105.4 m were loose sediments (mainly silty clay), which are interbedded by two main aquifer layers at a depth of 27–32 m and 76–91 m (silt and fine sand). During the drilling of the borehole, undisturbed cores were taken from different strata, and the lithology of the strata was mapped through by borehole logging. The physical properties of the soils along the borehole are summarized in Table 1 based on the results of the core tests. The thermal conductivity from the cores were obtained by lab testing of undisturbed soil samples using Hot Disk TPS 2500 S.

3.2. In-situ thermal conductivity investigation

In the borehole, we conducted the TRT, DTRT, and ATRT to measure the in-situ thermal conductivity. For these, double U-pipes were buried to a depth of 95 m, whereas the deeper borehole could not be accessed due to collapse after drilling. The water-filled tubes in the borehole were backfilled by a grout consisting of medium-sized sand, and at the ground surface, a bentonite-cement was used for sealing to the top. The boreholes were equipped with permanent CMHC which were pasted on the outer wall of the pipes for the ATRT (Fig. 2a and b). In comparison to applications of DTRT, where cables are temporally inserted into the pipes, the CMHCs attached to the outer face of the pipes are in closer contact with the surrounding soil (Fig. 2c), so that the heat can be better transferred and the thermal conditions of the soil are accessed directly.

Firstly, a thermal response test was conducted that was interpreted with (DTRT) and without (TRT) the CMHC for temperature sensing. Heating was applied by warming up the circulating fluid in BHE on-site with an average of 74 W/m. The test lasted for 82 h, covering three

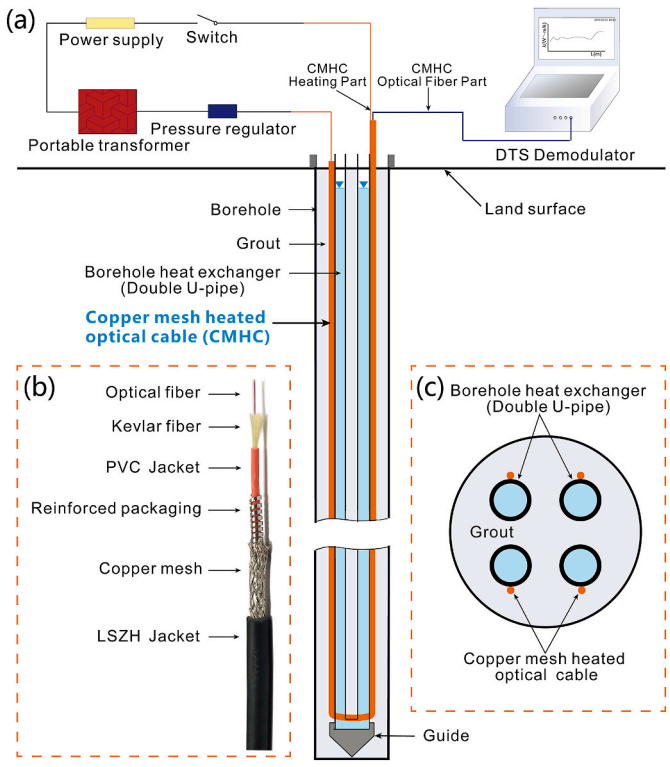

Fig. 2. Schematic diagram of ATRT system. (a) Test setup of ATRT in Changzhou site, (b) Image of CMHC, (c) Cross-section of the borehole shows the locations of CMHC and BHE in the borehole.

periods: (i) the initial 22 h served as a preparatory temperature measurement period without heating; (ii) the next 48 h represents the heating period, followed by (iii) a 12 h period recording the recovery. A thermal resistance thermometer recorded the inlet and outlet water temperature, and a DTS demodulator (NZS-DTS-A03) logged the vertical temperature distribution. The spatial resolution of NZS-DTS-A03 was 0.41 m, its temperature resolution was 0.01 K, and the measurement interval was set to 30 s.

The ATRT was conducted six months later. By inducing the electric current in the CMHC, the cable served as the heating source with a constant heating power of 26 W/m. The ATRT lasted 3 h which also had three periods: (i) 0.6 h for the initial temperature measurement, (ii) 1.6 h for the heating phase, and (iii) 0.8 h for inspecting the recovery.

3.3. Data analysis process

All tests (TRT, DTRT, ATRT) are interpreted by applying the infinite line source model [50–52]. The underlying heat transfer equation assumes only one-dimensional heat conduction:

$$\frac{\partial T}{\partial t} = \frac{\lambda \partial^2 T}{pc\ \partial x^2} \tag{1}$$

where T is temperature, K; t is heating time, s; λ is the thermal conductivity, W/mK; ρ is the density of soil, kg/m^3; c is the specific heat capacity of the soil, J/kgK. For the TRT, Equation (1) assumes depth-independent radial heat transport and thus averages in depth. Though for DTRT and ATRT, this equation is applied stepwise along the borehole depending on the vertical resolution measured temperature.

When the line heat source is a cylinder with a radius r_0, and the initial temperature distribution is constant, the temperature rise of the line heat source in different locations can be obtained by:

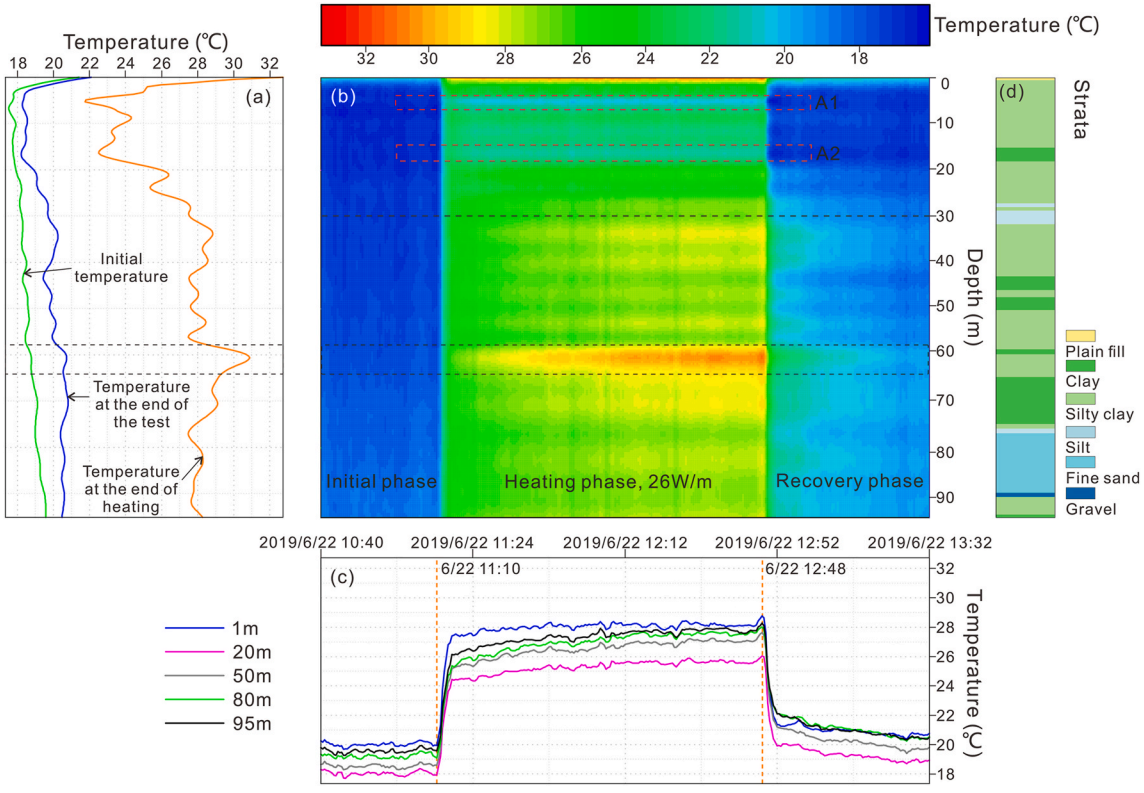

Fig. 3. Temperature variation of CMHC during ATRT. (a) Temperature distribution along the borehole at three specific times (i.e. the initial condition, the end of heating, the end of test), (b) Temperature variation with both time and depth obtained by DTS, (c) Temperature variation curves at five specific depths, which are at the shallow surface (1 m), the bottom of the borehole (95 m), the aquitards (20 m, 50 m), and the aquifer (80 m), (d) Stratigraphic subdivision of the borehole.

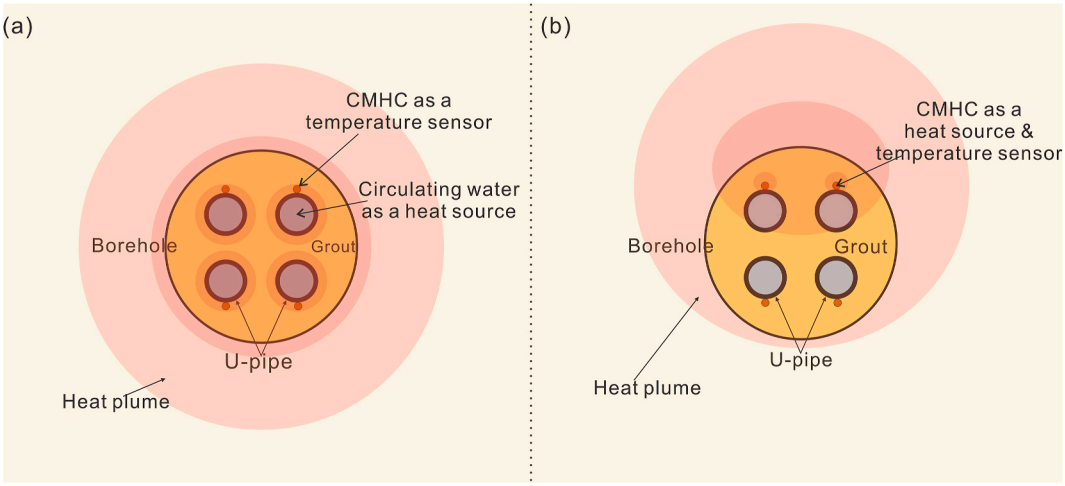

Fig. 4. Schematic diagram of heat transfer. (a) TRT & DTRT, (b) ATRT.

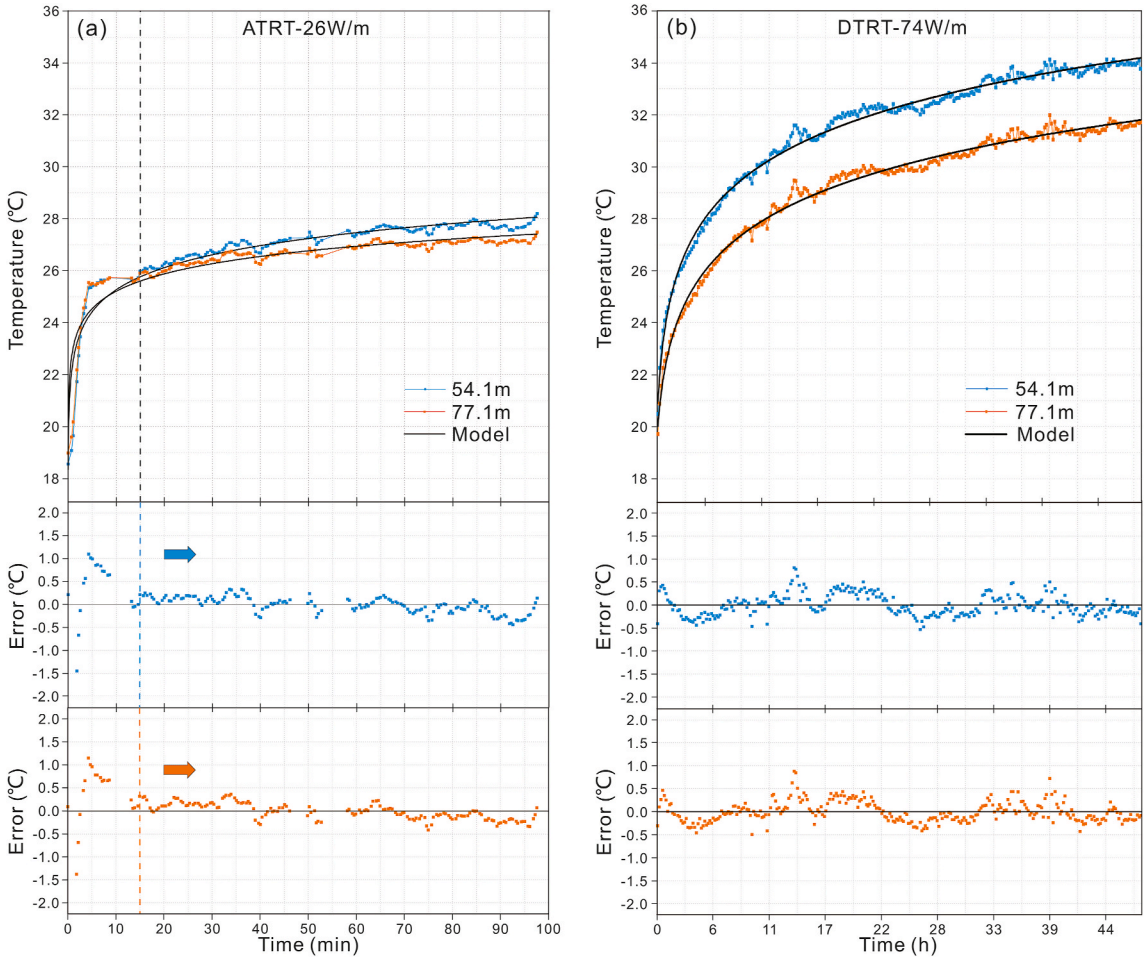

Fig. 5. Comparison of ATRT and DTRT on temperature rise. (a) Measured and modeled temperature response at the depth of 54.1 m and 77.1 m of ATRT, (b) Measured and modeled temperature response at the depth of 54.1 m and 77.1 m of DTRT.

$$\Delta T(\tau_0, t) = \frac{q}{4\pi\lambda}\left[\mathrm{In}\left(\frac{4at}{r_0^2 C}\right) + \frac{\tau_0^2}{4at} + o\left(\frac{\tau_0^2}{4at}\right)^2\right] \quad (2)$$

where ΔT is temperature rise in K; r_0 is the radius of the heat source (m); q is heating power (W/m); a is the thermal diffusivity (m^2/s); and $C = e^{\gamma}$, with γ being the Euler–Mascheroni constant.

When r_0 is small enough and t is long enough, the second-order expressions and infinitely small quantity of the higher-order term in Equation (2) can be neglected. The basic equation for measuring the thermal conductivity reads:

$$\lambda = \frac{q}{4\pi k} \quad (3)$$

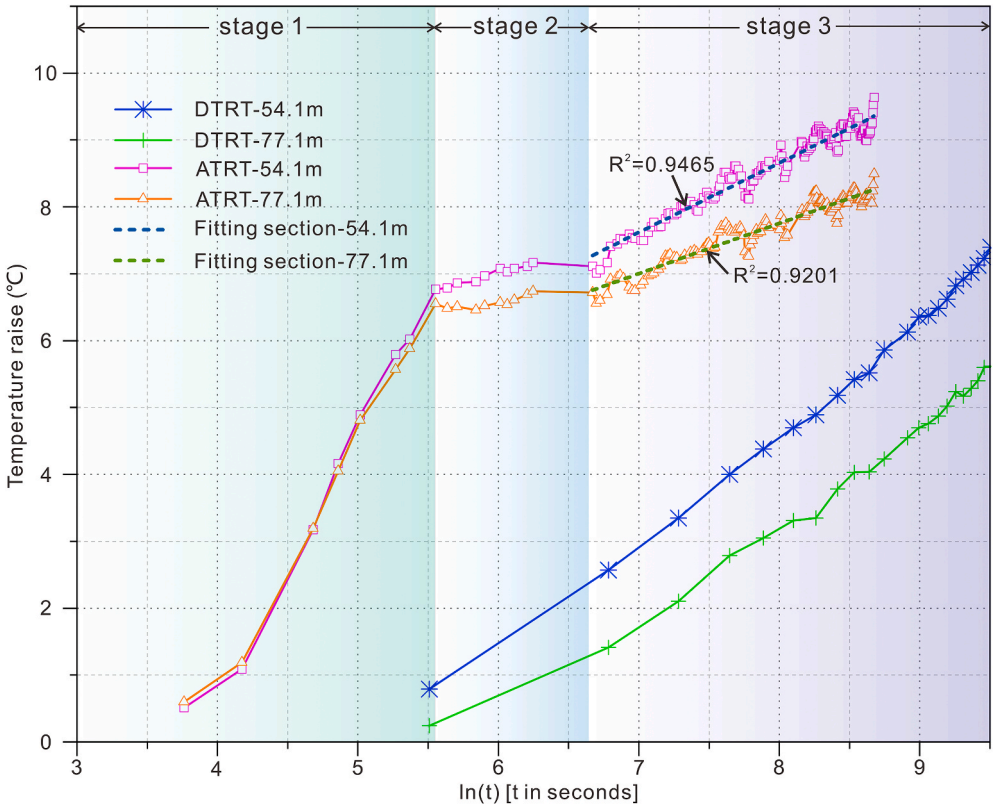

Fig. 6. Measured temperature raise for ATRT and DTRT in the initial heating period.

where k is the slope of the measured date plotted as ΔT-lnt curve, $k = d\Delta T/dlnt$, which can be graphically determined by curve fitting and minimizing the root mean squared error (RMSE). Theoretically, the slope is constant for conduction in ideal radially homogeneous media. In the field test, the line heat source and the target soils are usually not in direct contact. Therefore, especially during the early test time, the recorded thermal responseΔT is influenced by any devices within the BHE such as heat source packaging, tubes, and grout. In practice, this bulk thermal effect of the borehole devices is expressed by computing the borehole resistance based on the observed early time behavior, whereas later temperature recordings are utilized for the determination of λ.

4. Results and discussions

4.1. TRT and DTRT based results

Based on the inlet and outlet temperature of the transducer pipe during the heating process, the average thermal conductivity of the ground, according to standard TRT interpretation, was calculated to be 2.268 W/mK. For the DTRT, the thermal conductivity of the strata in different depths (stepwise moving window at a resolution of 0.41 m) is calculated by a least-squares batch fitting of Equations (2) and (3). The derived average thermal conductivity of the strata is 2.186 W/mK. The difference between DTRT and TRT results is thus less than 4%, indicating that both TRT and DTRT results are similarly reliable.

4.2. Analysis of the temperature measurements of ATRT

For the ATRT, the temperature evolution along the CMHC during the whole test is shown in Fig. 3. Before the heating phase, the initial temperature distribution along the pipe was recorded. The undisturbed vertical trend presents a typical temperature-time curve in summer time as expected, with a strong increase in the top few meters due to the coupling of ground temperature with the conditions in the atmosphere (Fig. 3a). The natural geothermal gradient along the borehole below a depth of 30 m is around 2.1 °C/100 m.

When starting to heat the optical cable with the copper mesh, there was a significant temperature rise measured by ΔT = 8–12 °C (Fig. 3b and c). At most depths, during the heating phase, the temperature rise of the cable goes through two phases, (iia) a rapid initial temperature rise followed by (iib) a phase of slow change afterwards. The temperature change is influenced by the surrounding soils of different depths and the groundwater flow. The trends for the shallow subsurface (1 m), the bottom of the hole (95 m), the low-permeable layers (20 m, 50 m), and the deeper aquifer layer (80 m) are plotted in Fig. 3c. It is notable that in the depth range of 0–30 m, there are relatively smaller temperature increases (phase iib) after the rapid initial temperature rise. Examples like regions A1 and A2 in Fig. 3b demarcate levels of small temperature change during the test. Since only conduction was considered when fitting Equations (2) and (3), the calculated thermal conductivity can be unreliable, likely due to the relatively poor coupling between soils and cable under low confining pressure and also the influence of groundwater flow. A similar result was reported by Luo et al. [36] who obtained a thermal conductivity of 60 and -60 W/mK if ignoring the effect of groundwater when conducted a DTRT in an 80 m borehole.

For the comparison of DTRT and ATRT, the strata in the depth range of 30–95 m with significant temperature changes are chosen (Fig. 3c). At the same power supply, the slower and smaller temperature rises indicate a larger thermal conductivity of the strata or groundwater flow due to the faster heat transfer [21]. In the range of 58–65 m, the temperature increases by around 12 °C. This is significantly higher than at other depth positions, indicating that here the heat is transmitted slowly and the strata have a relatively small thermal conductivity.

According to the heat transfer Equation (2), the degree of heat diffusion is crucial for calculating the thermal conductivity of the thermal response test. To illustrate this for the TRT, DTRT, and ATRT, a

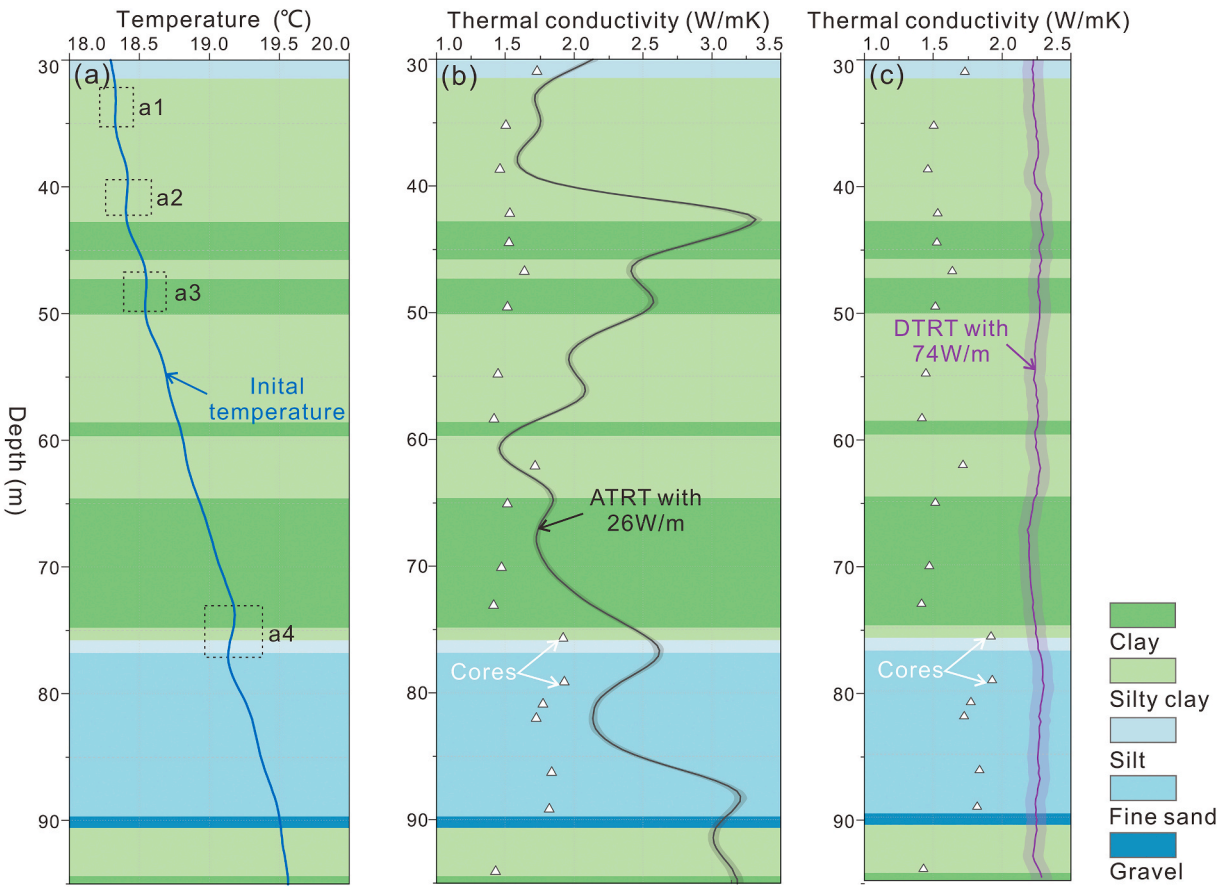

Fig. 7. Ground temperature distribution and calculated thermal conductivity distribution obtained by ATRT and DTRT. (a) Initial undisturbed ground temperature at the borehole, (b)The thermal conductivity and its 95% confidence interval estimated for ATRT, (c) The thermal conductivity and its 95% confidence interval estimated for DTRT.

schematic cross section through the borehole heat exchanger is shown in Fig. 4. Depending on the heat source a specific thermal anomaly could evolve. For the ATRT, the heat source has a smaller specific heat capacity and area, and less heat is dissipated in the heat source. When more heat enters the soils, the temperature rise information can reflect the thermal conductivity of the soils in shorter time. According to the calculation principle of the infinite line source model, the temperature measured by the copper mesh heated optical cable in the DTRT & ATRT defaults to the heat source temperature. Theoretically, the method of integrating the temperature measuring fiber into the heated copper mesh in the ATRT test is more in line with the calculation of the hot wire method, which will cause less error.

For inspecting the differences between ATRT and DTRT in more detail, two points in different strata are chosen. Fig. 5 presents the trends in silty clay at 54.1 m and fine sand at 77.1 m for both ATRT and DTRT. The thermal response curves of the two methods fit well to Equation (2), and the residual distribution is ±0.5 °C. It can be seen that the overall error of ATRT is smaller than that of DTRT in the results of fitting equations to temperature-time data acquired at two depths of 54.1 m and 77.1 m by DTRT and ATRT, Fig. 4 also reveals that the overall model fits the ATRT data better than the DTRT, so the overall ATRT results appear to be more stable and reliable than those of the DTRT. For the ATRT, however, there is a large variation in the initial stage of heating; the calculated error of up to 1 °C shows a big difference between the temperature change and the overall change trend during this period, which cannot be well reproduced by the line source equation (Equation (2)). The large error in the initial stage can be explained by the low thermal conductivity of the sheathing material of CMHC, which was caused by a rapid accumulation of heat. This also indicates that the calculation of the ATRT result should discard the temperature in the early stage in order to reduce the error.

The *T-ln(t)* curve of the heating phase temperature as a function of time at depths of 54.1 m and 77.1 m is plotted in Fig. 6. It can be seen that the typical temperature trend of the ATRT is different from that of the DTRT based on the data in the initial period, affected by the different heat source and temperature sensor structures. In the case of using CMHC, the temperature change of ATRT can be divided into three stages:

(1) The measured temperature quickly increases, and it is caused by the small thermal conductivity of the CMHC coat (i.e. LSZH). The computed thermal conductivity λ of LSZH is generally less than 0.5 W/mK.
(2) When the heat transfers through the jacket material, the slope of the temperature changes and strongly declines due to the presence of the grout and water-filled tubes.
(3) As the slope of temperature change stabilizes in the soils surrounding the borehole, the slope of the temperature versus logarithm time tends to be stable. Obviously, for insight into the ambient soil properties, the ATRT is ideally interpreted by this last stage that can be easily separated from the previous ones with strong influence from borehole properties.

4.3. ATRT based results and the verification

The thermal conductivity distribution and its 95% confidence interval in the range of 30–95 m for the ATRT are shown in Fig. 7b. The thermal conductivity varies from 1.5 W/mK to 3.5 W/mK. As is

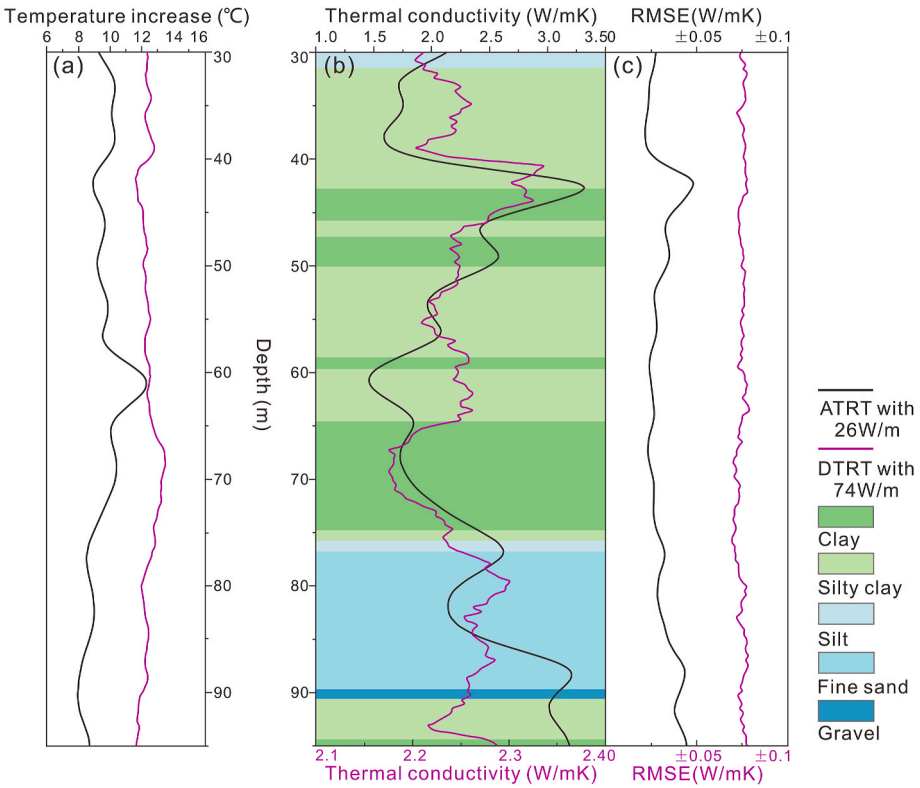

Fig. 8. Comparison of ATRT and DTRT. (a)The temperature rise of ATRT and DTRT, (b) Comparison of ATRT and DTRT thermal conductivity curves, (c) RMSE at two tests.

Table 2
Comparison of ATRT and related thermal response test concepts.

Test Methods	Heat source material	Heating time (h)	Heating power (W·m^{-1})	Energy consumption (kWh·m^{-1})	Temperature rise (°C)
ATRT (this study)	Copper mesh	1.6	26	0.0416	8–12
DTRT (this study)	water	48	74	3.5520	8.5–14
des Tombe (2018)	Copper core	115.2	20	2.3040	3–6
Vélez Márquez (2018)	Copper core	135.6	9.9	1.3424	4–6
Vieira (2017)	Multiple copper core	84	28	2.352	/
		96	23.1	2.3136	/
Galgaro (2018)	Multiple copper core	5	24.1	0.1205	/

expected, there are small thermal conductivities derived for the low permeable strata while large thermal conductivities denote the strongly groundwater-influenced levels. It is revealed that the thermal conductivities λ obtained in the lab (expressed in triangles) are generally smaller than the ATRT and DTRT results. Note that the influence of advection is not resolved by the standard line source approach. Therefore, the derived values of λ are effective values, which are more or less enhanced by the accelerated heat flux from flowing groundwater (Fig. 7b and c). The results for the ATRT seem to be more consistent with the core test measurements, mainly reflected in the magnitude of the change, except for the range of 40 m–50 m and 85 m–95 m, showing a high consistency. It is speculated that there is more significant groundwater flow in these two depth ranges. For the undisturbed initial ground temperature of Fig. 7a, the temperature profile of the abnormal temperature gradient (a1-a4) illustrates the effect of certain groundwater seepage [53,54].

The results of ATRT and DTRT are compared in Fig. 8. With the use of CMHC, the ATRT obtained a temperature increase of 8–12 °C at a heating power of 26 W/m, while the corresponding DTRT temperature rise was 11.5–13.5 °C at the input power of 74 W/m (Fig. 8a). The ATRT result showed good agreement with that obtained by DTRT, as the average thermal conductivity of ATRT and DTRT was 2.2455 and 2.2464 W/mK, respectively, with an error of less than 1% (Fig. 8b). The RMSE of the thermal conductivity based on ATRT is between 0 and 0.05 W/mK while that of DTRT is between 0.05 and 0.1 W/mK (Fig. 8c). As illustrated in Fig. 8b, it can be seen that the variation of the thermal conductivity obtained by ATRT is significantly larger than that of DTRT although they have similar trends in different strata. The variation of thermal conductivity along the borehole calculated by ATRT is more reasonable compared with the core results (Fig. 7b) because groundwater flow generally increases the value of the measured thermal conductivity. Compared to DTRT, ATRT can be more sensitive to thermal conductivities of different strata and hence has the potential to provide a more accurate measurement.

4.4. Thermal conductivity evaluation efficiency of ATRT

For the thermal response test, according to Equation (2), the relation between applied heating power and temperature rise is fundamental for the thermal conductivity calculation, and thus due to the disturbances in the field, a small temperature rise brings more uncertainty. Changing the heating power or the heat source (e.g. calcium chloride solution or metal heat source) can affect the efficiency of the thermal response test [55]. Higher power can bring higher temperature rise and a suitable structure

can make the most use of the consumed energy [37]. With the use of CMHC, the ATRT obtained a temperature increase of 8–12 °C at a heating power of 26 W/m, while the corresponding DTRT temperature rise was 11.5–13.5 °C at an input power of 74 W/m. This displays that ATRT using CMHC with lower specific heat capacity can be more efficient than the DTRT. In other words, ATRT can obtain the same temperature raise but with lower energy cost than DTRT.

Des Tombe et al. [56] and Vélez Márquez et al. [37] reported the use of heating cables as heat sources. The former fit a single composite fiber-optic cable and a heating cable together, and used thinner push-rods to reach a depth of 45 m. The latter placed heating cable and fiber optical cable separately into different pipes of the double U-pipe. Aside from these, Vieira et al. [31] and Galgaro et al. [38] reported the use of a hybrid cable integrating a copper and fiber optical component. Their method further improved the test efficiency and reduced the test time to 5 h. Table 2 summarizes the energy consumption of each test reported in these previous studies as well as for our application. Copper is commonly selected as the heating wires because it can be used for long-distance testing. Compared with other heating wires based thermal response tests, ATRT using CMHC obtains the highest temperature rise at similar heating powers. Obviously, the ATRT greatly reduces the energy consumption per unit length (0.0416 kWh/m). The use of CMHC further improves heating efficiency and reduces the test duration to 1.6 h.

5. Conclusions

The feasibility of actively heated fiber optics based thermal response test (ATRT) was demonstrated in a field test accompanied with conventional TRT and DTRT. The presented results reveal that the novel method can provide a reliable thermal conductivity distribution along the borehole but with lower energy cost and a shorter test time than reported for related field methods. This offers a more efficient thermal property evaluation in the field, both technically and economically. Rather than using a hybrid cable built up by a separate heating and temperature sensing cable, the presented use of a copper mesh heated optical cable (CMHC) improves the reliability of temperature sensing in the borehole.

The experience from the field study is worthwhile to identify the opportunities by the ATRT. The findings, however, also show that there are several aspects that need further attention. Therefore, future work is required on optimal heating time and power, the effect of groundwater flow, the effect of borehole size, and the installation of a single cable without the presence of conventional U-pipes. Additionally, the active distributed temperature sensing applied in ATRT has also the potential to be further developed for soil moisture and groundwater flow velocity measurement.

CRediT authorship contribution statement

Bo Zhang: Methodology, Validation, Visualization, Writing - original draft. **Kai Gu:** Conceptualization, Methodology, Writing - review & editing. **Bin Shi:** Conceptualization, Supervision, Writing - review & editing. **Chun Liu:** Investigation, Methodology. **Peter Bayer:** Data curation, Writing - review & editing. **Guangqing Wei:** Methodology, Validation. **Xülong Gong:** Resources, Validation. **Lei Yang:** Resources, Validation.

Declaration of competing interest

The authors declare that they have no known competing financial interests or personal relationships that could have appeared to influence the work reported in this paper.

Acknowledgements

The authors acknowledge the National Natural Science Foundation of China (NSFC, No. 41427801, 41761134089, 41977217), the Key Project of Nanjing University Technology Innovation Fund (SC-2019-101), the Changzhou Urban Geological Survey Project and the German Research Foundation (No. 2850/3–1) for their critical financial support.

Abbreviations

ATRT	Actively heated fiber optics based thermal response test
BHE	Borehole heat exchanger
CMHC	Copper mesh heated optical cable
DTRT	Distributed thermal response test
DTS	Distributed Temperature Sensing
ETRT	Enhanced thermal response test
RMSE	Root mean square error
TRT	Conventional thermal response test

Nomenclature

T	Temperature (^{o}C)
t	Time (s)
λ	Thermal conductivity (W/mK)
ρ	Density of fluid (kg/m^3)
c	Specific heat capacity of soil (J/kgK)
ΔT	Temperature rise (^{o}C)
r_0	Radius of heat source (m)
q	Heating power (W/m)
a	Thermal diffusivity (m^2/s)
γ	Euler–Mascheroni constant
k	Slope of curve
R_b	Thermal borehole resistance (Km/W)

Appendix A. Supplementary data

Supplementary data to this article can be found online at https://doi.org/10.1016/j.rser.2020.110336.

References

[1] Bayer P, Attard G, Blum P, Menberg K. The geothermal potential of cities. Renew Sustain Energy Rev 2019;106:17–30. https://doi.org/10.1016/j.rser.2019.02.019.
[2] Yang H, Cui P, Fang Z. Vertical-borehole ground-coupled heat pumps: a review of models and systems. Appl Energy 2010;87:16–27. https://doi.org/10.1016/j.apenergy.2009.04.038.
[3] Luo J, Rohn J, Xiang W, Bertermann D, Blum P. A review of ground investigations for ground source heat pump (GSHP) systems. Energy Build 2016;117:160–75. https://doi.org/10.1016/j.enbuild.2016.02.038.
[4] Baglivo C, D'Agostino D, Congedo PM. Design of a ventilation system coupled with a horizontal air-ground heat exchanger (HAGHE) for a residential building in a warm climate. Energies 2018;11:2122. https://doi.org/10.3390/en11082122.
[5] Bayer P, de Paly M, Beck M. Strategic optimization of borehole heat exchanger field for seasonal geothermal heating and cooling. Appl Energy 2014;136:445–53. https://doi.org/10.1016/j.apenergy.2014.09.029.
[6] Ciriaco AE, Zarrouk SJ, Zakeri G. Geothermal resource and reserve assessment methodology: overview, analysis and future directions. Renew Sustain Energy Rev 2020;119:109515. https://doi.org/10.1016/j.rser.2019.109515.
[7] Mogensen P. Fluid to duct wall heat transfer in duct system heat storages. Doc Counc Build Res 1983:652–7.
[8] Spitler JD, Gehlin SEA. Thermal response testing for ground source heat pump systems - an historical review. Renew Sustain Energy Rev 2015;50:1125–37. https://doi.org/10.1016/j.rser.2015.05.061.
[9] Zhang C, Guo Z, Liu Y, Cong X, Peng D. A review on thermal response test of ground-coupled heat pump systems. Renew Sustain Energy Rev 2014;40:851–67. https://doi.org/10.1016/j.rser.2014.08.018.
[10] Javadi H, Mousavi Ajarostaghi SS, Rosen MA, Pourfallah M. Performance of ground heat exchangers: a comprehensive review of recent advances. Energy 2019;178:207–33. https://doi.org/10.1016/j.energy.2019.04.094.
[11] Ashrae BAI, Design E. ASHRAE handbook-HVAC applications (SI). Am soc heating, refrig air-conditioning eng inc, atlanta, USA. 2011.
[12] Smith M, Perry R. In situ testing and thermal conductivity testing. Proc. In: 1999 GeoExchange tech. Conf. Expo, Oklahoma, USA; May, 1999. p. 16–9.
[13] Bujok P, Grycz D, Klempa M, Kunz A, Porzer M, Pytlik A, et al. Assessment of the influence of shortening the duration of TRT (thermal response test) on the

precision of measured values. Energy 2014;64:120–9. https://doi.org/10.1016/j.energy.2013.11.079.
[14] Gehlin S, Hellström G. Recent status of in-situ thermal response tests for BTES applications in Sweden. 2000 Proc Terrastock 2000:159–64.
[15] Pasquier P. Interpretation of the first hours of a thermal response test using the time derivative of the temperature. Appl Energy 2018;213:56–75. https://doi.org/10.1016/j.apenergy.2018.01.022.
[16] Borinaga-Treviño R, Pascual-Muñoz P, Castro-Fresno D, Blanco-Fernandez E. Borehole thermal response and thermal resistance of four different grouting materials measured with a TRT. Appl Therm Eng 2013;53:13–20. https://doi.org/10.1016/j.applthermaleng.2012.12.036.
[17] Wagner V, Bayer P, Kübert M, Blum P. Numerical sensitivity study of thermal response tests. Renew Energy 2012;41:245–53. https://doi.org/10.1016/j.renene.2011.11.001.
[18] Tang F, Nowamooz H. Sensitive analysis on the effective soil thermal conductivity of the Thermal Response Test considering various testing times, field conditions and U-pipe lengths. Renew Energy 2019;143:1732–43. https://doi.org/10.1016/j.renene.2019.05.120.
[19] Wagner V, Blum P, Kübert M, Bayer P. Analytical approach to groundwater-influenced thermal response tests of grouted borehole heat exchangers. Geothermics 2013;46:22–31. https://doi.org/10.1016/j.geothermics.2012.10.005.
[20] Fujii H, Okubo H, Itoi R. Thermal response tests using optical fiber thermometers. GRC 2006 Annu. Meet. Geotherm. Resour. Our Energy Futur. 2006:545–51.
[21] Fujii H, Okubo H, Nishi K, Itoi R, Ohyama K, Shibata K. An improved thermal response test for U-tube ground heat exchanger based on optical fiber thermometers. Geothermics 2009;38:399–406. https://doi.org/10.1016/j.geothermics.2009.06.002.
[22] Acuña J, Palm B. Distributed thermal response tests on pipe-in-pipe borehole heat exchangers. Appl Energy 2013;109:312–20. https://doi.org/10.1016/j.apenergy.2013.01.024.
[23] Acuña J, Mogensen P, Palm B. Distributed thermal response test on a U-pipe borehole heat exchanger. In: Effstock 2009. 11th int. Conf. Therm. Energy storage, stock. Acad. Conf. Publ.; 2009.
[24] Acuña J, Mogensen P, Palm B. Distributed thermal response tests on a multi-pipe coaxial borehole heat exchanger. HVAC R Res 2011;17:1012–29. https://doi.org/10.1080/10789669.2011.625304.
[25] Acuña J, Palm B. A novel coaxial borehole heat exchanger: description and first distributed thermal response test measurements. Proc. World Geotherm. Congr. 2010:25–9.
[26] Cao D, Shi B, Zhu H-H, Wei G, Bektursen H, Sun M. A field study on the application of distributed temperature sensing technology in thermal response tests for borehole heat exchangers. Bull Eng Geol Environ 2019;78:3901–15. https://doi.org/10.1007/s10064-018-1407-2.
[27] Franco A, Conti P. Clearing a path for ground heat exchange systems: a review on thermal response test (TRT) methods and a geotechnical routine test for estimating soil thermal properties. Energies 2020;13:2965. https://doi.org/10.3390/en13112965.
[28] Wilke S, Menberg K, Steger H, Blum P. Advanced thermal response tests: a review. Renew Sustain Energy Rev 2020;119:109575. https://doi.org/10.1016/j.rser.2019.109575.
[29] Dornstädter J, Heidinger P, Heinemann-Glutsch B. Erfahrungen aus der Praxis mit dem Enhanced Geothermal Response Test (EGRT). Geothermics 2008;11:2008.
[30] Huber H, Arslan U. Geothermal field tests with forced groundwaterflow. Standford Geotherm. Work. 2012:5.
[31] Vieira A, Alberdi-Pagola M, Christodoulides P, Javed S, Loveridge F, Nguyen F, et al. Characterisation of ground thermal and thermo-mechanical behaviour for shallow geothermal energy applications. Energies 2017;10. https://doi.org/10.3390/en10122044.
[32] Freifeld BM, Finsterle S, Onstott TC, Toole P, Pratt LM. Ground surface temperature reconstructions: using in situ estimates for thermal conductivity acquired with a fiber-optic distributed thermal perturbation sensor. Geophys Res Lett 2008;35:3–7. https://doi.org/10.1029/2008GL034762.
[33] Raymond J, Robert G, Therrien R, Gosselin L. A novel thermal response test using heating cables. World Geotherm Congr 2010;25–29:1–8. April Bali, Indones 2010.
[34] Raymond J, Lamarche L. Development and numerical validation of a novel thermal response test with a low power source. Geothermics 2014;51:434–44. https://doi.org/10.1016/j.geothermics.2014.02.004.
[35] Raymond J, Lamarche L, Malo M. Field demonstration of a first thermal response test with a low power source. Appl Energy 2015;147:30–9. https://doi.org/10.1016/j.apenergy.2015.01.117.
[36] Luo J, Rohn J, Xiang W, Bayer M, Priess A, Wilkmann L, et al. Experimental investigation of a borehole field by enhanced geothermal response test and numerical analysis of performance of the borehole heat exchangers. Energy 2015;84:473–84. https://doi.org/10.1016/j.energy.2015.03.013.
[37] Vélez Márquez MI, Raymond J, Blessent D, Philippe M, Simon N, Bour O, et al. Distributed thermal response tests using a heating cable and fiber optic temperature sensing. Energies 2018;11:3059. https://doi.org/10.3390/en11113059.
[38] Galgaro A, Pasquier P, Schenato L, Cultrera M, Dalla Santa G. Soil thermal conductivity from early TRT logs using an active hybrid optic fibre system. 2018. https://doi.org/10.22488/okstate.18.000023.
[39] Bakker M, Caljé R, Schaars F, van der Made K, de Haas S. An active heat tracer experiment to determine groundwater velocities using fiber optic cables installed with direct push equipment. Water Resour Res 2015;51:2760–72. https://doi.org/10.1002/2014WR016632.
[40] Cao D-F, Shi B, Wei G-Q, Chen S-E, Zhu H-H. An improved distributed sensing method for monitoring soil moisture profile using heated carbon fibers. Measurement 2018;123:175–84. https://doi.org/10.1016/j.measurement.2018.03.052.
[41] He H, Dyck MF, Horton R, Ren T, Bristow KL, Lv J, et al. Development and application of the heat pulse method for soil physical measurements. Rev Geophys 2018;56:567–620. https://doi.org/10.1029/2017RG000584.
[42] Maldaner CH, Munn JD, Coleman TI, Molson JW, Parker BL. Groundwater flow quantification in fractured rock boreholes using active distributed temperature sensing under natural gradient conditions. Water Resour Res 2019;55:3285–306. https://doi.org/10.1029/2018WR024319.
[43] Read T, Bour O, Bense V, Le Borgne T, Goderniaux P, Klepikova MV, et al. Characterizing groundwater flow and heat transport in fractured rock using fiber-optic distributed temperature sensing. Geophys Res Lett 2013;40. https://doi.org/10.1002/grl.50397. 2055–9.
[44] Sayde C, Buelga JB, Rodriguez-Sinobas L, El Khoury L, English M, van de Giesen N, et al. Mapping variability of soil water content and flux across 1–1000 m scales using the A ctively Heated Fiber Optic method. Water Resour Res 2014;50:7302–17. https://doi.org/10.1002/2013WR014983.
[45] Sayde C, Gregory C, Gil-Rodriguez M, Tufillaro N, Tyler S, van de Giesen N, et al. Feasibility of soil moisture monitoring with heated fiber optics. Water Resour Res 2010;46. https://doi.org/10.1029/2009WR007846.
[46] Sayde C, Thomas CK, Wagner J, Selker J. High-resolution wind speed measurements using actively heated fiber optics. Geophys Res Lett 2015;42:10064–73. https://doi.org/10.1002/2015GL066729.
[47] Bense VF, Read T, Bour O, Le Borgne T, Coleman T, Krause S, et al. Distributed T emperature S ensing as a downhole tool in hydrogeology. Water Resour Res 2016;52:9259–73. https://doi.org/10.1002/2016WR018869.
[48] Peel MC, Finlayson BL, McMahon TA. Updated world map of the Köppen-Geiger climate classification. Hydrol Earth Syst Sci 2007;11:1633–44. https://doi.org/10.5194/hess-11-1633-2007.
[49] Huang S. Geothermal energy in China. Nat Clim Change 2012;2:557–60. https://doi.org/10.1038/nclimate1598.
[50] Carslaw HS, Jaeger JC. Conduction of heat in solids. Clarendon press; 1992.
[51] Cortes DD, Martin AI, Yun TS, Francisca FM, Santamarina JC, Ruppel C. Thermal conductivity of hydrate-bearing sediments. J Geophys Res Solid Earth 2009;114:1–10. https://doi.org/10.1029/2008JB006235.
[52] Huetter ES, Koemle NI, Kargl G, Kaufmann E. Determination of the effective thermal conductivity of granular materials under varying pressure conditions. J Geophys Res E Planets 2008;113:1–11. https://doi.org/10.1029/2008JE003085.
[53] Bredehoeft JD, Papaopulos IS. Rates of vertical groundwater movement estimated from the Earth's thermal profile. Water Resour Res 1965;1:325–8. https://doi.org/10.1029/WR001i002p00325.
[54] Anibas C, Buis K, Verhoeven R, Meire P, Batelaan O. A simple thermal mapping method for seasonal spatial patterns of groundwater–surface water interaction. J Hydrol 2011;397:93–104. https://doi.org/10.1016/j.jhydrol.2010.11.036.
[55] Noorollahi Y, Saeidi R, Mohammadi M, Amiri A, Hosseinzadeh M. The effects of ground heat exchanger parameters changes on geothermal heat pump performance – a review. Appl Therm Eng 2018;129:1645–58. https://doi.org/10.1016/j.applthermaleng.2017.10.111.
[56] des Tombe BF, Bakker M, Smits F, Schaars F, van der Made KJ. Estimation of the variation in specific discharge over large depth using distributed temperature sensing (DTS) measurements of the heat pulse response. Water Resour Res 2019;55:811–26. https://doi.org/10.1029/2018WR024171.